

A mathematical model of the coupled mechanisms of cell adhesion, contraction and spreading

Franck J. Vernerey · Mehdi Farsad

Received: 11 November 2011 / Revised: 23 January 2013 / Published online: 6 March 2013
Springer-Verlag Berlin Heidelberg 2013

Abstract Recent experimental work on cell spreading is highly dependent on the combination of its biochemical and the mechanical properties of the environment in which it is located. The dynamic of cell spreading is a key process in development of tissue engineering, such as bone healing, wound contraction, stem cell maintenance and angiogenesis. To better understand and highlight the physical aspects of cell spreading and contraction, we present a mathematical model for the coupling of cell spreading and contraction at the cell edge and dynamic of cell-cell junctions (in epithelium) enabling cell-cell adhesion. The evolution of cell-cell junctions is modeled as a mixture of fluid, polymer and filament, which can change mass and generate contraction. In particular, we identify the role of the cell-cell junctions in the dynamic of cell-cell adhesion and gene expression. The present approach is able to model the development of cell-cell adhesion complex through the mechanotransduction of cell-cell junctions, known in epithelium. After identifying the governing equations for the dynamic of cell-cell junctions and spreading, we introduce a numerical solution based on the finite element method, combined with a level set formulation. Numerical simulations show that the proposed model is able to capture the dependence of cell spreading and contraction on cell-cell adhesion, stiffness, and chemotaxis. The model is a good agreement between model prediction and experimental observations, highlighting the mechanical processes underlying the coupled mechanisms of contraction, adhesion and spreading of adherent cells.

Mathematical Subject Classification 92B05 · 74S05 · 74F20

F. J. Vernerey (✉) · M. Farsad
Department of Civil, Environmental and Architectural Engineering,
University of Colorado, Boulder, USA
e-mail: franck.vernerey@colorado.edu

mechanics of β -catenin activation in the mechanical force have been addressed by a series of models, some based on purely mechanical aspects (Foccardi and Venerè, 2012; Sameni et al. 2009) and some based on biochemical aspects, including signalling pathways (Cielekogl-Scholer et al. 2005). At the cellular level, the development of global β -catenin, organ activation and adhesion have recently been the object of a formalization (Dehpande et al. 2008) based on empirical relationships between the mechanical displacement, activation of β -catenin, and in equilibrium. A similar continuum approach is also introduced in the

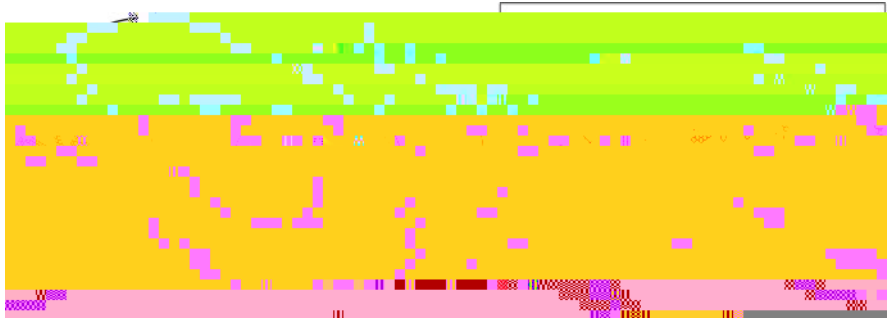


Fig. 1 Gene al congl a ion of an ci c; la cell loca ed on an elā ic, i b a e i h a ep ē en a ion of the h ee fo m of ac in con ide ed in h j , i d; globē la , lamē oē , and bē ndled (ē ē , ē ē , ē ē)

he ac in c, o kele on a a mi ē e of foē majo con i ē en, ē ep ē en ing he c, o ol and ac in in h ee diffe en fo m : globē la , lamē oē , and bē ndled (Fig. 1). In i, globē la fo m, ac in eā il, diffe ē h oē ghoē he c, o kele on and hē , ma, be ē ep ē en ed a a i id phā ē in he p ē en, i d. In i, lamē oē fo m, ho ē ē , ac in

$$\dots + \dots \left(\frac{v}{\dots} + \frac{v}{\dots} \right) + \dots + \left(\frac{\dots}{\dots} + \frac{\dots}{\dots} \right) = 0 \quad (7)$$

$$\left(\frac{v}{\dots} + \frac{v}{\dots} \right) + \dots + \left(\frac{\dots}{\dots} + \frac{\dots}{\dots} \right) + \left(\frac{\dots}{\dots} + \frac{\dots}{\dots} \right) = 0 \quad (8)$$

$$\dots + \left(\frac{v}{\dots} + \frac{v}{\dots} \right) + \dots = 0 \quad (9)$$

$$\dots + \frac{1}{1 + \dots} \left(\dots + \dots + \dots \right) = 0 \quad (10)$$

he e $\mathbf{I} = 1$, i he c, o ol p e, e, \mathbf{T} he pa ial, e, in he pa, i e c, o kele on and \mathbf{T} he pa ial, e, ind ced b, e, . We no e he e ha he e m, pa, i e c, o kele on— a i, ed on a b oad, e n e a i ep e n, a n i mbe of po, ble componen, con ibi ing o he cell el a i. Thi incl d e fo i n ance, mic o i b i e, in e media e. lamen, and he memb ane loca ed on op and he bo om of a plana cell. A, i ming, mall defo ma ion (a i n a e pical l e, han 10% in he p oblem of in e e), a linea el a i c e la ion can be, ed o d e c i be he pa, i e c, o kele on e po e:

$$= \frac{1}{2}(\dots + \dots) + \dots = \dots, \text{ and } = \dots \quad (13)$$

he e $= 1$ and $= \dots$. The ma e ial pa ame e, and ep e n he Yo: ng' mod i l e, and Poj, on' a io, e pec i el, hile he adial and ci c i mfe en ial linea a i n and a e el a ed o he adial d i placemen b, e = $\frac{1}{\dots}$ and $= \frac{1}{\dots}$. A d i c i, ed in mo e de ail in [Ve ne e, and Fa, ad \(2011\)](#), he pa ial, e, \mathbf{T} of e, be, i p o po i onal o he ol i me f a c i o n and a i e f o m o diffe en o i ce : ac i e con ac ion and pa, i e el a i c e po e. We he e fo e i e:

$$= \dots (1 + \dots) = \dots, \quad (14)$$

he e he coef i c i e n \dots deno e he, ifne, of, e, be, hile he con ac ile e, * i he e i l of ac o m, o i n c o, b i dge d, nam i c a he, a come ic le el ([Ve ne e, and Fa, ad 2011](#)). Al ho: gh, a come e fo ce i kno n o depend on he a e of con ac ion a p edic ed b, he Hill model ([Hill 1938](#)), e cho e o neglec h i a pec fo he p e n, i d, and con ide ha he con ac ile, e, i con an and e f i al o ha fo i nd in a, a e of i ome ic con ac ion. Thi a, i mp i o n i mo i a ed b, he fac ha cell, p eading i a, lo p o e, compa ed o he cha ac e i c ime, cale of c o, b i dge d, nam i c and i he e fo e i n e n i i e o he a e of elonga ion of, a come e. Final l, fo ce e f i lib i k m in he mi i e follo, f o m he balance of linea momen i m. Unde a i, mme ic and plane, e, condi o n, h i, jeld:

$$\frac{\dots}{\dots} + \frac{1}{\dots}(\dots) = 0 \quad (15)$$

In abo e e f i a ion, deno e he hickn e, of he cell and ep e n, he d i b i e ed ac ion fo ce on he memb ane a i i n g f o m he in e ac ion i h he i nd e l i n g, i b, a e i a focal adhe ion. While h i fo ce i applied a he bo om of a cell h o: gh i, memb ane, i i e f i i alen o con ide i a a angen ial bod, fo ce applied o he c, o kele on b i n oking plane, e, a, i mp i o n . To a nall, cha ac e i e he beha i o of he i nd e l i n g, i b, a e, i i i e, e f i l o no e ha i, hickn e, i, i all m, ch la ge han ha of cell. In h i, i i a ion, e, a i a ion a e e pec ed in a

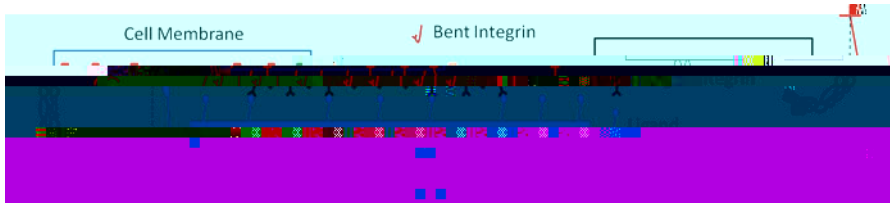


Fig. 3 In equilibrium ligand complex: a ligand, low-affinity in equilibrium, and bound to high-affinity in equilibrium, b in equilibrium, a, c, e. The relative placement between the two is of equilibrium ligand complex

$$\mu = \mu \tag{17}$$

are in equilibrium. A low concentration of ions, and low-affinity in equilibrium can typically be achieved at a dilute solution in the lipid membrane, which has a high chemical potential in equilibrium with the high-affinity in equilibrium, as follows:

$$\mu = \mu_0 + \ln\left(\frac{\dots}{0}\right) \tag{18}$$

where μ_0 and \dots are the free energy and concentration of low-affinity in equilibrium, and a condition, respectively. The chemical stability of high-affinity in equilibrium is known to depend on the amount of energy of the system, as described by (Shem et al. 2005; Peol et al. 2003; Tan et al. 2003). In the case of the equilibrium phase, a high-affinity in equilibrium, cell concentration (from the system) is high, as a result of the high-affinity in equilibrium which end of the system, stability. To capture this phenomenon, it is important to consider the influence of high-affinity in equilibrium in the condition: high-affinity in equilibrium (high concentration) and high-affinity in equilibrium (high concentration) of the high-affinity in equilibrium. Following Lauffenberger and Linderman (1993), the concentration of bound in equilibrium can be expressed as a function of the total ligand concentration as follows:

$$= \frac{\dots}{1 + \dots} \tag{19}$$

This expression shows how the high-affinity in equilibrium concentration end of the system of equilibrium of the high-affinity in equilibrium. The stability of equilibrium in equilibrium is high, as a result of the following form of the chemical potential (Dehpande et al. 2008):

$$\mu$$

he e μ_0

To characterize the membrane elasticity, the following constitutive law is proposed (Vennemann and Fardad 2011):

$$\mathbf{T} = \frac{1}{2} \mathbf{C} : \mathbf{E} \quad \text{and} \quad \mathbf{D} = \mathbf{0} + \frac{1}{2} \mathbf{C} : \mathbf{E}^2 \quad (29)$$

Here \mathbf{C} is the deformation gradient, \mathbf{E} is the second-order strain tensor, and \mathbf{D} is the third-order tensor of the cell membrane. The mechanical equilibrium of the membrane is given by the balance of forces and moments (Vennemann and Fardad 2011; Vennemann and Fardad 2011):

$$\mathbf{T} \cdot \mathbf{n} = \mathbf{0} \quad \text{and} \quad \mathbf{D} \cdot \mathbf{n} = \mathbf{0} \quad (30)$$

where \mathbf{T} is the second-order stress tensor, \mathbf{n} is the outward normal to the cell membrane, and \mathbf{D} is the third-order stress tensor. It can be shown that the equilibrium conditions are satisfied if the constitutive law (30) is used in which the stress tensors are defined on the boundary.

2.3 Membrane porosity and cell growth

Let us now consider the phenomenon of membrane porosity from a physical point of view. This aspect of cell mechanics is known in the literature as being active in polymerization at the cell edge and membrane porosity (Cielie et al. 2007; DiMilla et al. 1991; O'Connell and Pechon 1985; Pollard and Borner 2003; Valloin et al. 2005; Wakayuki et al. 2003; Xiong et al. 2010). Similar to the previous section, the chemo-mechanical coupling can be mathematically added by considering the chemical equilibrium of the membrane on the cell edge and how it is affected

The total change of free energy during an equilibrium cycle can then be expressed by adding contributions from eqs 1 and 2. This yields:

$$\mu = (2.1). \quad (34)$$

We are now in a position to give the chemical potential of ac in monomer, in the aggregated form accounting for the effect of membrane and in equilibrium, (Hill 1981):

$$\mu = \mu_0 + \mu = \mu_0 + (2.1) \quad (35)$$

Note that the change in free energy from the presence of physical forces added to the original chemical potential μ_0 , since μ is independent of μ_0 , is mediated by the ac in equilibrium during a polymerization step. When the equilibrium is reached, the chemical potential of G-ac in and ac in filament, (aggregated ac in) are equal ($\mu = \mu$) and we obtain:

$$\mu_0 + (2.1) = \mu_0 + (2.1) \text{ in } h_2 = \frac{\mu_0}{h_2} \quad (36)$$

Here, we have the fact that the equilibrium free energy of ac in monomer and ac in filament are equal, being $\mu = 0$ in (31)

While the coefficient β generally a function of the magnitude of participating force (see discussion in Hill 1981), we consider here a constant ($\beta = 1/2$) for simplicity. In order to determine the physical force affecting on- and off-axis cells, using (39) and (31), it is then possible to obtain the velocity of cell spreading (or the rate of accretion) along the membrane:

$$v = \frac{0}{\dots} \exp\left(-\frac{(\dots)^2}{\dots}\right) \quad (41)$$

where v is the force dependent concentration of G-actin in a cell, defined in (38). The above equation characterizes the behavior of cell spreading. In particular, one can see from (41) that the membrane velocity is independent of the growth rate while the peeling force increases. Since the inherent peeling force is directly related to cell contraction, (41) characterizes the coupling between cell contraction and spreading: the more contraction, the faster the spreading. For the same reason,

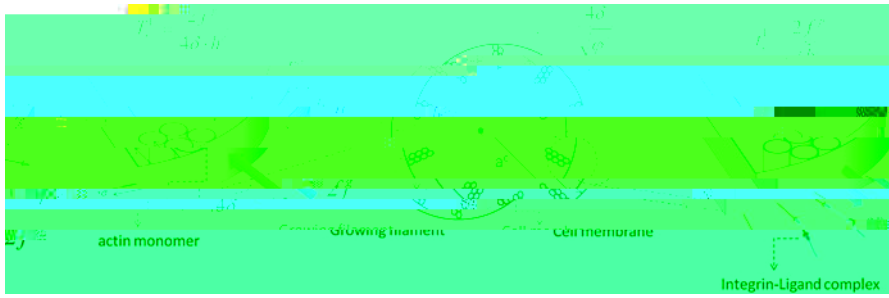


Fig. 5 Relation hip between the membrane porosity, ion force σ and σ_c and in equilibrium force σ_c and membrane tension

pulling force σ_c may be high of a σ_c the equilibrium force of diameter in equilibrium action on a portion of the cell edge h or length h the average distance between adjacent actin filaments. This length can then be calculated from the actin molecule fraction at the cell edge $b_c = 4 / \dots$ (Fig. 5). This leads to the estimation of the pulling force σ_c :

$$\sigma_c = \frac{1}{2} \dots = \frac{2}{\dots} \dots \tag{44}$$

the equilibrium in equilibrium force at the cell perimeter and the product of the effective area on which the in equilibrium action helps the polymerization of a single filament. Note that (43) and (44) provide a clear relationship between the mechanics of in equilibrium, the membrane porosity σ_c and the area of cell growth in (41).

The cell membrane is given in terms of the inelastic function and and finally the deformation of the cell is given in terms of the knowledge of internal displacement. The above equations may be determined through the following equilibrium conditions in the piezoelectricity:

Chemical equilibrium

$$\text{Series } \mu = \mu \quad \text{in} \quad (45)$$

$$\text{Acin } \mu = \mu \quad \text{on} \quad (46)$$

$$\text{Cell membrane } \mu = \mu \quad \text{in} \quad (47)$$

Mass conservation

$$\text{Coul } \left(\frac{v}{x} + \frac{v}{x} \right) + \dots + \left(\frac{v}{x} + \frac{v}{x} \right) = 0 \quad (48)$$

$$\text{Mile } \left(\frac{v}{x} + \frac{v}{x} \right) + \dots + \left(\frac{v}{x} + \frac{v}{x} \right) + \left(\frac{v}{x} + \frac{v}{x} \right) = 0 \quad (49)$$

$$\text{In eqn } \left(\frac{v}{x} + \frac{v}{x} \right) + \left(\frac{v}{x} + \frac{v}{x} \right) + \left(\frac{v}{x} + \frac{v}{x} \right) = 0 \quad (50)$$

Mechanical equilibrium

$$\text{Cell } \left(\frac{v}{x} + \frac{v}{x} \right) + \left(\frac{v}{x} + \frac{v}{x} \right) - \dots = 0 \quad (51)$$

$$\text{Sub } \left(\frac{v}{x} + \frac{v}{x} \right) + \dots = 0 \quad (52)$$

The equilibrium are complemented by the boundary conditions (corresponding to the above differential equations) and initial conditions, specifying the state of the cell at the beginning of the simulation. The conditions are, which have the cell and sub are a e initial deformation and displacement:

$$f(x, 0) = 0 \quad f(x, 0) = 0 \quad f(x, 0) = 0 \quad (53)$$

In addition, it is assumed that the composition of the cell consists of 25% volume fraction of element, comprising the piezoelectric, 5% volume fraction of actin monomer, and no initial piezoelectric (reference for heteromeric, are given in Table 1).

$$f(x, 0) = 0.25 \quad f(x, 0) = 0.05 \quad f(x, 0) = 0 \quad (54)$$

and all in equilibrium are originally in the following state (see Table 1 for reference):

$$f(x, 0) = 5^{-15} \quad f(x, 0) = 0 \quad (55)$$

Concerning the boundary conditions, we assume that the external force of Coul and actin monomer, across the cell membrane and no load originally in equilibrium are allowed on the membrane. In using Eqs. (11) and (26), we can hence write:

Table 1 Pa ame e, i, ed in he, im; la ion

De ni ion	S mbol	Val; e	Uni	Refe encę
-----------	--------	--------	-----	-----------

C; o; ol; ol; me f ac ion

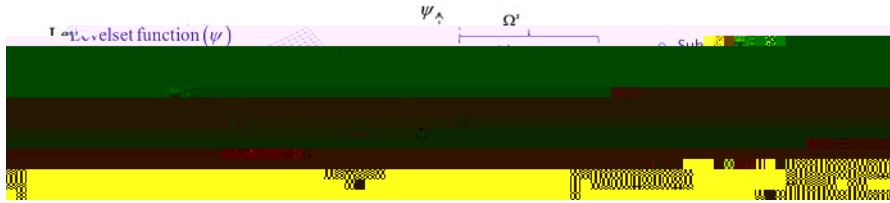


Fig. 6 Illustration of the levelset function defining the cell boundary and the degree of freedom associated with nodes in the computational domain

the element and a defined the element, in the membrane. Finally, the above term of element is coupled with the global element (41) in order to determine the motion of the cell boundary in time. The numerical approach, outlined (48–52) is described below.

3.1 Cell-based element formulation

In order to determine the partial and time evolution of the material field, the physical domain (epithelial cell and cell-based membrane) be discretized in a finite number of elements and nodes. A potential issue in the present problem is the cell

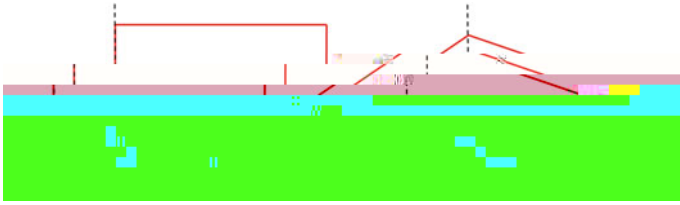


Fig. 7 a

Here $e = 1, 2, 3$ denote the local node number for each element and the element $\bar{\mathbf{u}}$ and $\bar{\mathbf{u}}$ correspond to longitudinal and shear degrees of freedom respectively for non-enriched elements. Substituting the finite element polynomials (58) in the weak form and linearizing the equations, one can show that the problem reduces to solving the following algebraic problem:

$$\mathbf{C}\dot{\mathbf{U}} + \mathbf{K} \mathbf{U} + \mathbf{F} = \mathbf{0} \tag{63}$$

Here \mathbf{U} denotes the vector containing global degrees of freedom, while \mathbf{C} , \mathbf{K} and \mathbf{F} are the damping matrix, stiffness matrix and force vector respectively (see Appendix A.2 for a more detailed explanation). Equations (63) are solved at each time step, using a Newmark-Raphon procedure and a backward Euler integration method, to compute the unknown field at each time step, as follows:

$$\mathbf{U} = \dot{\mathbf{U}} \tag{64}$$

where $\dot{\mathbf{U}}$ denotes the time increment. Upon obtaining a solution at time increment n , the method consists of computing the average $\bar{\mathbf{U}}$ at the next time step:

$$\bar{\mathbf{U}}(n+1) = \bar{\mathbf{U}}(n) + \dot{\mathbf{U}} \tag{65}$$

where the average $\bar{\mathbf{U}}$ is computed for each element by substituting Eqs. (64) and (65) into Eq. (63). This leads to the following equation:

$$\left(\mathbf{C}_{+1} + \mathbf{K}_{+1} \right) \cdot \dot{\mathbf{U}} = \left(\mathbf{F}_{+1} + \mathbf{C}_{+1} \cdot \bar{\mathbf{U}}_{+1} \right) \tag{66}$$

The average is then updated in the form of the vector \mathbf{U} in the next time step.

3.2 Cell growth and cell death

To model cell growth, from the equilibrium equations at each time step, one can determine the pressure and membrane tension force appearing in (41). Since the cell adhesion is defined in terms of the cell-cell tension, the change in time can imply the definition of the additional cell-cell tension (Dai et al. 2008):

$$\sigma = \sigma + \dot{\sigma} = 0 \tag{67}$$

where the cell boundary velocity is computed in (41). Defining the cell-cell adhesion tension (i.e. $\sigma = 1$), one can find the pressure of the cell-cell tension at time step $n+1$ as:

$$\sigma_{+1} = \sigma + \dot{\sigma} \tag{68}$$

Go h picall, in ol_e he ç ea ion of ne ma e ial poin, , ho e compo i ion i
 nkno n, a he cell bo: nda. I j h, necç, a o make, ome a, i mp ion ega ding
 he, a e of he mi e a he ne cell edge in e m of he con i e n; ol e
 f ac ion. To e e he con i i of bo h a con i i m eld and i, de i a i e d e ing
 cell g o h, a eali ic a, i mp ion (A e hian 2007) con i, of app o ima ing a eld

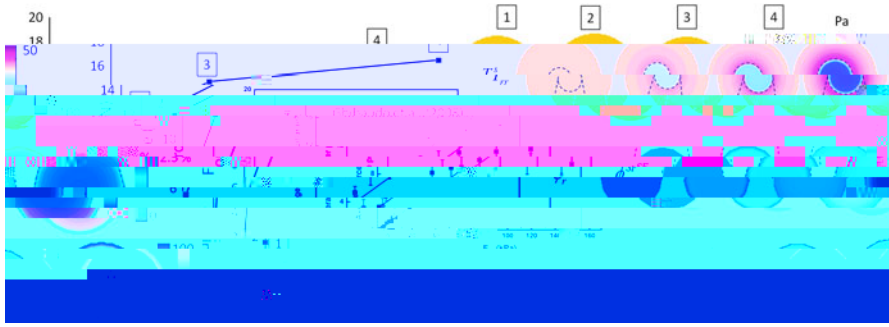


Fig. 8 Relationship between cell contraction and cell adhesion forces, respectively. The model predicts a nonlinear relationship between contraction and adhesion forces, in agreement with experimental micropillar data (Ghibaudo et al. 2008). For comparison purposes, the relationship between the total force in the dynamic equilibrium of the whole computed in equilibrium conditions by the numerical model and the applied force is plotted. The evolution of adhesion forces in the adhesion mechanism of the cell, respectively, in the adhesion and the concentration of high affinity receptors, is shown for different adhesion forces.



Fig. 9 Evolution of pulling force, membrane tension force and cell adhesion force

Cell adhesion is provided by the clustering of integrins in ligand complexes. The chemical equilibrium is described in Sec. 2.2. Cell contraction, respectively, adhesion, depends on the membrane and the internal forces, respectively, the adhesion forces. When ligand receptors are present, the integrins are binding to the ligands, respectively, leading to the activation of the signaling pathway (22). This explains the activation

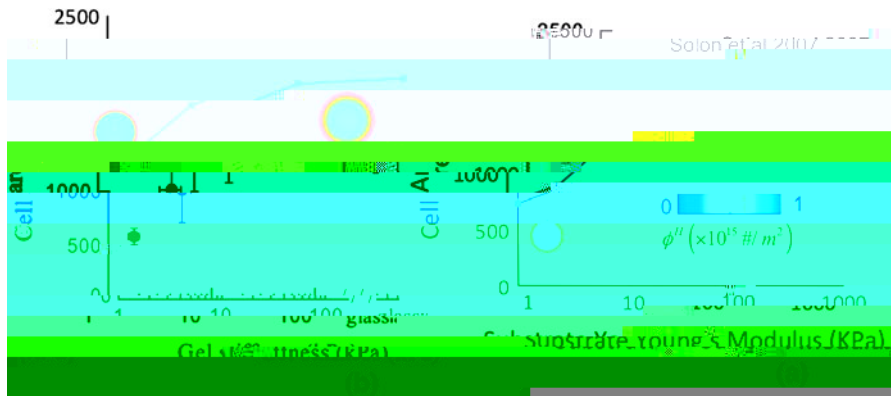


Fig. 10 Change of cell area and high-affinity binding concentration in response to a difference in ligand concentration and compression in the experimental setting of Solon et al. (2007)

The effective preloading area, preloading force and membrane stretching force are depicted as a function of time. It is seen that the preloading area is a function of the difference between σ_c and σ_m , which has a negative value. The velocity of preloading becomes negligible. Another effect of the preloading force is to increase the area of preloading by acting on the actin filament. The model hypothesizes that the area of preloading is in both cell area and preloading area in compression and, therefore, the area of preloading becomes larger and one more of the high in Fig. 8.

The model predicts that the effective mechanical area is nonlinearly related and dependent on the area of preloading and ligand density. We note that the order of the model by comparing numerical prediction and experimental measurement from the literature.

4.2 Effect of area of preloading on cell area

Experimental studies on fibroblasts have shown that cell area (Solon et al. 2007) increases with the area of preloading in a nonlinear fashion (Fig. 10). The effective ligand concentration depends on the ligand concentration in the cell, preloading only affected by preloading. To increase cell preloading, the area of an original cell containing a ligand of surface area $A_0 \approx 600 \mu^2$ in which no preloading and high-affinity binding are present. Since high-affinity binding is originally of equilibrium, the effective area depends on the preloading force, in equilibrium ligand adsorption and cell preloading have an effect on each other.

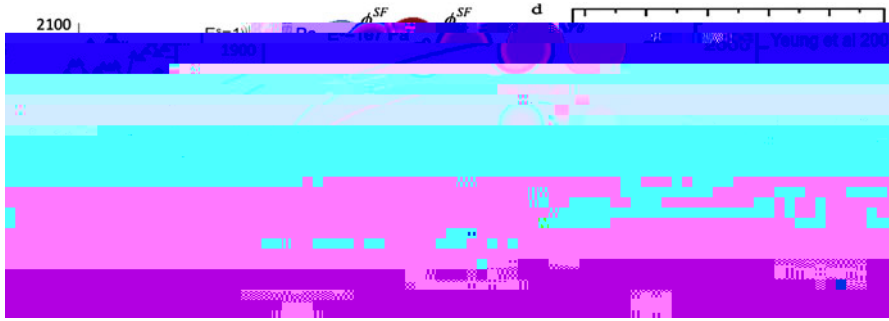


Fig. 11 a Change of cell area and ϵ , β and γ of the polymer ion density ρ for different ϵ , β , γ , α , δ , and η and b dependence of ϵ , β , γ of Young et al. (2005)

a limit, which depends on the mechano-elastic properties of the polymer ion. First, ϵ , β , γ , α , δ , η and ρ are all, each a maximum concentration, which limits the concentration a cell can experience on its own and hence the pulling force. Second, according to (41), the area of, pulling is controlled by the competition between pulling and the ϵ pulling force. As observed in Fig. 9, the ϵ pulling force, while originally weak, increases a much faster rate than the pulling force and eventually becomes the dominating factor; hence, an end of cell, pulling.

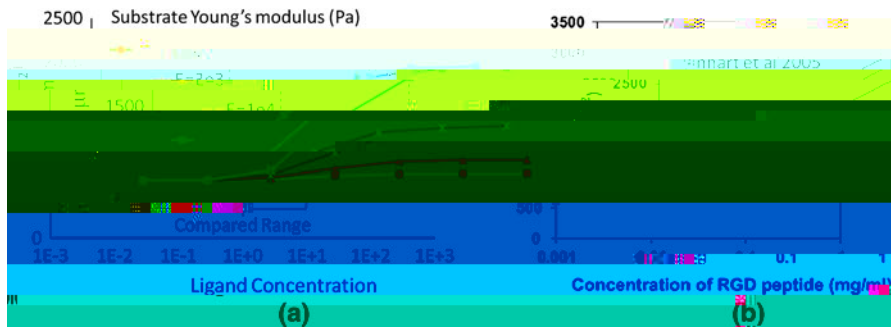


Fig. 12 Change of cell area, adhesion force for different ligand concentration, and comparison in the peptide immobilization of Reinhart-King et al. (2005)

the cell area is a linear function of ligand density in this concentration range from 0.001 to 1 mg/ml. To know the behavior of the proposed model compared to the experimental data, we considered a cell length on a $1 \mu\text{m}$ scale of gelatin, stiffness, and varied the ligand concentration from 0.001 to 1,000 ligand/ μm^2 . As depicted in Fig. 12, the model predicted a non-linear relationship between ligand density and cell area. While this result may seem contradictory to the experimental data, the area of the plane for the observed displacement F_{ij} , is, should be noted that the change of ligand concentration considered in the immobilization mechanism has a higher range of peptide immobilization. In fact, if one compares the same concentration range, the model predicted increase in cell area is close to the linear relationship seen in the experiment. For the more realistic of higher range, model prediction is a perfect indicator and it is known that cell area cannot increase and measure each mechanism, regardless of the concentration of ligand. Similarly, when no ligand is present, cell area may converge to a small value. This is the fact that cell area has a high proportion of ligand density, and also in this. Finally, the increase of cell area with ligand concentration can be explained on the basis of (22). On the one hand, when ligand density is high, in equilibrium cannot achieve the $1 \mu\text{m}$ scale; the probability of the presence of a peptide force and the associated increase in cell area. On the other hand, when ligand density is high, cell cannot achieve the $1 \mu\text{m}$ scale and generate a connection; the probability of area, also, is a

ligand attachment on the plasma membrane is promoted by the increase in phospholipid and endocytosis both concentration and adhesion, respectively. Finally, the phenomenon of polarization of the cell of an insect is due to the opposite forces: the increase in phospholipid at the edge of the cell and the stretching and bending of the cell membrane. These mechanisms have been presented in this article as a dynamically consistent framework of fundamental principles, which

and enforcing the fact that $\dot{y} = \dots$, we obtain the following equation for \dot{y} :

$$\dot{y} = \frac{1}{1} \left[-(1 + \dots)(1 - 2 \dots) \left(\dots + \dots \right) \right] \quad (71)$$

where \dots and \dots are the Young's modulus, and Poisson's ratio of the actin filament network. The relationship between the Lamé constants, appearing in (70) is given below:

$$\dots = \frac{\mu'(3 + 2\mu')}{\mu'}; \quad \text{and} \quad \dots = \frac{\dots}{2(\dots + \mu')} \quad (72)$$

We now impose the divergence of the velocity field \mathbf{v} for incompressibility in the equation of mass balance (4-6). For a hydrodynamical problem, the divergence of $\mathbf{v} = \dots + \dots + \dot{y}$ has to be imposed to be zero and we obtain the following equation:

$$\dot{y} = \frac{1}{1} \left[\dots (1 + \dots)(1 - 2 \dots) \left(\dots + \dots \right) \right] \quad (73)$$

from (71), we can see that:

- Ci, elekoglı -Schole, G, Wa, ne O. A, No, akd I, Mej, e a JJ, Sch, a, e MA, Mogilne A (2005) Model of co, pled, an, ien change of, ac, ho, adhe, ion and, e, be, alignmen in endo helial cell. e ponding o, hea, e, . J Theo Biol 48:569-585
- Cq, a KD, Lee EJ, Holme, JW (2003) Ce, a ing alignmen and anj o, op, and enginee ing hea, i, e: role of bo, nda, condi ion in a model h ee-dimen, ional ci, l, e, em. Tij, e Eng 9(4):567-577
- C ame LP (1997) Molec, la mechanj m of ac in-dependen, e, og ade, o in lamellipodia of mo ile cell. E on Biq, ci 2:d26-270
- C ame LP, Mi chj on TJ, The io JA (1994) Ac in-dependen, mo ile fo, e, and cell mo ili. C, l, . Opin Cell Biol 6:82-86
- Damien C, The, M, Ch, Y-S, Di, fo, S, Thie, J-P, Bo, ne, M, Na, o, P, Mahade, an L (2007) The, i, ni, e, al d, namic of cell, p eading. C, l, Biol 17:694-699
- Damien C,2.2(LP)-191.686.4(M k ich250-34.8(M)28.6(a285.20ich2506-352.130)-9.3(1A pl)-2506-R.)] mMdel

- Shemę h T, Geige B, Be, had k, A, Ko. lo, MM (2005) Focal adhe ion a mechanę en o, : a ph ical mechanj m. P oc Na l Acad Sci 102:12383-12388
- Solon J, Le, en al I, Sengę p a K, Geo gę PC, Janme, PA (2007) Fib obla adap a ion and, iffneę, ma ching o, of elą ic, i b a e. Bioph, J 93(12):4453-4461
- S ameno, ic D, La opo; lo KA, Pi en j A, S; ki BE (2009) Mechanical, abili de e mineę, e, be and focal adhe ion o ien a ion. Cell Mol Bioeng 2(4):475-485
- Tan JL, Tien J, Pi one DM, G a, DS, Bhad i aj; K, Chen CS (2003) Cell l ing on a bed of mic oneedle : an app oach o j ola e mechanical fę ce. P oc Na l Acad Sci 100(4):1484-1489
- T, i da Y, Yą i ake H, I hijima A, Yanagida T (1996) To, ional igidi of, ingle ac in. Mlamen, and ac in ac in bond b eaking fę ce i nde o, ion meą i. ed di ec l, b, in i. o mic omanip; la ion. P oc Na l Acad Sci 93:12937-12942
- Vallo on P, Dan, e G, Bohne S, Mej e J-J, Ve kho, k, AB (2005) T acking e. og ade o in ke a o cę : ne, f om he f on. Mol Biol Cell 16:1223-1231